RKKY interaction and the nature of the ground state of double dots in parallel

M. Kulkarni and R. M. Konik

Phys. Rev. B **83**, 245121 — Published 23 June 2011

DOI: 10.1103/PhysRevB.83.245121

The RKKY Interaction and the Nature of the Ground State of Double Dots in Parallel

M. Kulkarni[1,2] and R. M. Konik[1]

[1] *Department of Condensed Matter Physics and Material Science, Brookhaven National Laboratory, Upton, NY 11973-5000, USA*

[2] *Department of Physics and Astronomy, Stony Brook University, Stony Brook, NY 11794-3800, USA*

(Dated: May 4, 2011)

We argue through a combination of slave boson mean field theory and the Bethe ansatz that the ground state of closely spaced double quantum dots in parallel coupled to a single effective channel are Fermi liquids. We do so by studying the dots' conductance, impurity entropy, and spin correlation. In particularly we find that the zero temperature conductance is characterized by the Friedel sum rule, a hallmark of Fermi liquid physics, and that the impurity entropy vanishes in the limit of zero temperature, indicating the ground state is a singlet. This conclusion is in opposition to a number of numerical renormalization group studies. We suggest a possible reason for the discrepancy.

PACS numbers: 73.63.Kv, 72.10.Fk, 71.27.+a, 02.30.1k

I. INTRODUCTION

Quantum dots provide a means to realize strongly correlated physics in a controlled setting. Because of the ability to adjust gate voltages which control both the tunnelling amplitudes between the dots and the connecting leads and the dots' chemical potential, quantum dots can be tuned to particular physical regimes. One celebrated example of said tuning was the first realization of Kondo physics in a single quantum dot,[1,2] obtained by adjusting the chemical potential of the dot such that the dot was occupied by one electron.

More generally, engineered multi-dot systems offer the ability to realize more exotic forms of Kondo physics. This was seen, for example, in the realization of the unstable fixed point of two-channel overscreened Kondo physics in a multi-dot system.[3] There has thus been considerable theoretical interest in double dots systems in different geometries, both in series (for example Refs. 5–10) and in parallel (for example Refs. 11–24). In this article we focus on the strongly correlated physics present on the latter geometry, in particular when there is no direct tunneling between the dots and the dots are not capacitively coupled. Such dot systems have been experimentally realized in numerous instances[25–27] (for other realizations of double dots in parallel see Refs. 28,29). Although the dots are not directly coupled, they are coupled through an effective Ruderman-Kittel-Kasuya-Yosida (RKKY) interaction. It is aim of this work to explore the nature of the RKKY interaction in parallel double quantum dots.

A straightforward application of the RKKY interaction as typically understood would lead one to believe that in a closely spaced double quantum dot with two electrons present, one on each dot, the RKKY interaction should lead to an effective ferromagnetic coupling between the dots. How should this coupling reveal itself in a transport experiment, the typical probe of a quantum dot system? If a ferromagnetic coupling is present, one expects the electrons on the two dots to bind into a spin-1 impurity. If the dots are coupled to a single effective lead, we obtain, in effect, an underscreened Kondo effect. As the temperature is lowered, the single effective lead will partially screen the spin-1 impurity to an effectively uncoupled spin-1/2 impurity. The ground state of the system will then be a non-Fermi liquid doublet. In particular at small temperatures and voltages, the conductance through the dot will be characterized by logarithms.[30] This scenario has been put forth in a number of NRG studies[13,14,16,17] and is implicit in a number slave boson studies[18–20] of double dots in parallel.

We present contrary evidence here that this scenario is not in fact applicable at least for temperatures below the Kondo temperature. We argue that the ground state of closely spaced double dots is instead a Fermi liquid singlet. These findings are consistent with those of Ref. 6. We do so using both the Bethe ansatz and slave boson mean field theory. It has been shown[11,12] that under certain conditions double dots in parallel admit an exact solution using the Bethe ansatz. This exact solution, following the approach introduced in Ref. 31, can be exploited to compute transport properties. In particular, the zero temperature linear response conductance can be computed exactly. Double quantum dots, however, only admit an exact solution provided their parameters satisfy certain constraints. To ensure that our finding of Fermi liquid behaviour is not an artifact of these constraints, we also study the parallel dot system using slave boson mean field theory. This allows one to study the sensitivity of our results to adding a second weakly coupled channel and to compute such quantities as the spin-spin correlation function, an object not directly computable in the Bethe ansatz.

The paper is organized as follows. In Section II we detail the double dot model that we are interested in studying together with the approaches (Bethe ansatz and slave boson mean field theory) that we employ in studying this system.

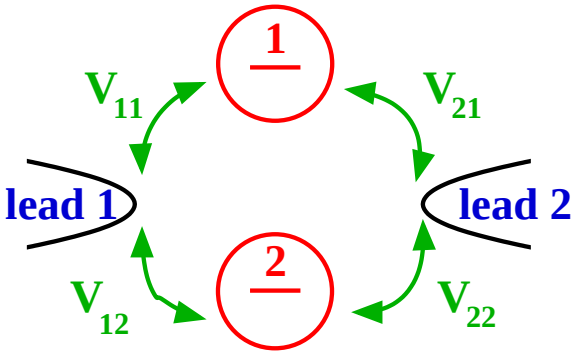

FIG. 1: A schematic of the double dot system.

In Section III we present results on the linear response conductance through the dots both at zero temperature and finite temperature. We show the zero temperature conductance obeys the Friedel sum rule, a hall mark of Fermi liquid physics. We also study the impurity entropy at finite temperature showing that it vanishes in the zero temperature limit indicating the presence of a singlet. Finally in this section, we present results (using slave boson mean field theory alone) of the spin-spin correlation function. Lastly, in Section IV, we discuss the implications of our results and suggest a way they can be reconciled with the conflicting NRG studies.

II. MODEL STUDIED

We study a set of two dots arranged in parallel with two leads. The Hamiltonian for this system is given by

$$\begin{aligned}\mathcal{H} &= -i\sum_{l\sigma}\int_{-\infty}^{\infty} dx c^{\dagger}_{l\sigma}\partial_x c_{l\sigma} + \sum_{\sigma\alpha} V_{l\alpha}(c^{\dagger}_{l\sigma\alpha}d_{\sigma\alpha} + \text{h.c}) \\ &+ \sum_{\sigma\alpha}\epsilon_{d\alpha}n_{\sigma\alpha} + \sum_{\alpha} U_{\alpha}n_{\uparrow\alpha}n_{\downarrow\alpha}. \end{aligned} \quad (1)$$

The $c_{l\sigma}$ specify electrons with spin σ living on the two leads, $l = 1, 2$. The $d_{\alpha\sigma}$ specify electrons found on the two dots $\alpha = 1, 2$. Electrons can hop from the leads to dots with tunneling strength $V_{l\alpha}$. The strength of the Coulomb repulsion on the two dots is given by U_{α}. We suppose that there is no interdot Coulomb repulsion and that tunneling between the two dots is negligible. A schematic of this Hamiltonian for the two dots is given in Fig. 1.

A. Bethe Ansatz

The above Hamiltonian can be solved exactly via Bethe ansatz under certain conditions. The set of constraints that we will be particularly interested in are as follows:

$$\begin{aligned} V_{1\alpha}/V_{2\alpha} &= V_{1\alpha'}/V_{2\alpha'}; \\ U_\alpha \Gamma_\alpha &= U_{\alpha'}\Gamma_{\alpha'}; \\ U_\alpha + 2\epsilon_{d\alpha} &= U_{\alpha'} + 2\epsilon_{d\alpha'}. \end{aligned} \tag{2}$$

The first of these conditions results in only a single effective channel coupling to the two leads. This occurs automatically when the dot hoppings are chosen to be symmetric and so is commonly found in the literature.[13,14,18,20–22,32] The second condition tells us that with $U_{1,2}$ fixed, $\epsilon_{d1} - \epsilon_{d2}$, is also fixed. We thus must move $\epsilon_{d1,2}$ in unison in order to maintain integrability. The final condition tells us that $\sqrt{U_i \Gamma_i}$, the bare scale governing charge fluctuations on the dots must be the same on both dots.

To solve this Hamiltonian we implement a map to even and odd channels, $c_{e/o} = (V_{1/2,\alpha} c_1 \pm V_{2/1,\alpha} c_2)/\sqrt{2\Gamma_\alpha}$ where $\Gamma_\alpha = (V_{1\alpha}^2 + V_{2\alpha}^2)/2$. Under the map, the Hamiltonian factorizes into even and odd sectors:

$$\begin{aligned} \mathcal{H}_e &= -i \sum_{l\sigma} \int_{-\infty}^{\infty} dx\ c_{e\sigma}^\dagger \partial_x c_{e\sigma} + \sum_{\sigma\alpha} \sqrt{2\Gamma_\alpha}(c_{e\sigma\alpha}^\dagger d_{\sigma\alpha} + \text{h.c}) \\ &\quad + \sum_{\sigma\alpha} \epsilon_{d\alpha} n_{\sigma\alpha} + \sum_\alpha U_\alpha n_{\uparrow\alpha} n_{\downarrow\alpha}; \\ \mathcal{H}_o &= -i \sum_{l\sigma} \int_{-\infty}^{\infty} dx\ c_{o\sigma}^\dagger \partial_x c_{o\sigma}, \end{aligned} \tag{3}$$

where, as can be seen, the odd sector decouples from the double dot. Using the Bethe ansatz[11,12] one can construct N-particle wave functions in the non-trivial even sector. These wavefunctions are characterized by N-momenta $\{q_i\}_{i=1}^N$ and M quantum numbers $\{\lambda_\alpha\}_{\alpha=1}^M$. The number of λ_α's mark the spin quantum number of the wave function: $S_z = N - 2M$. Together the λ_α's and q_i's satisfy the following set of constraints:

$$\begin{aligned} e^{iq_j L + i\delta(q_j)} &= \prod_{\alpha=1}^{M} \frac{g(q_j) - \lambda_\alpha + i/2}{g(q_j) - \lambda_\alpha - i/2}; \\ \prod_{j=1}^{N} \frac{\lambda_\alpha - g(q_j) + i/2}{\lambda_\alpha - g(q_j) - i/2} &= -\prod_{\beta=1}^{M} \frac{\lambda_\alpha - \lambda_\beta + i}{\lambda_\alpha - \lambda_\beta - i}, \end{aligned} \tag{4}$$

where $g(q) = \frac{(p - \epsilon_{d\alpha} - U_\alpha/2)^2}{2\Gamma_\alpha U_\alpha}$. These equations are identical to the set of constraints for a single dot[42,43] but for the form of the scattering phase $\delta(q)$:

$$\delta(q) = -2\tan^{-1}\left(\sum_\alpha \frac{\Gamma_\alpha}{q - \epsilon_{d\alpha}}\right). \tag{5}$$

We will focus in this paper on computing transport properties in linear response. At zero temperature we can use the Bethe ansatz to access such transport quantities exactly.[12,31] We will also use the Bethe ansatz to obtain an excellent quantitatively accurate prediction (in comparison with NRG) for the finite temperature linear response conductance (see Refs. 12,31 for the Bethe ansatz computation of the finite temperature linear response conductance for a single dot and for the comparable NRG, Ref. 46).

The Bethe ansatz can be exploited to develop certain approximations that allow one to compute certain non-equilibrium quantities, in particular, the out-of-equilibrium conductance[31] and the noise[33] in the presence of a magnetic field. In order to obtain at least qualitatively accuracy, the presence of a magnetic field is a necessity. With a magnetic field the Bethe ansatz for a single dot correctly predicts such features as the positioning of the peak in the differential magnetoconductance[33] as say measured in carbon nanotube quantum dots.[4] In the absence of a magnetic field, the Bethe ansatz inspired approximation breaks down however.[33] We will, again, not consider the double dots out-of-equilibrium in this work.

B. Slave Boson Mean Field Theory

We also study the Hamiltonian (1) using a slave-boson mean field theory, a well-known technique, applicable at sufficiently low temperatures.[47] The starting point is the same Hamiltonian (1) and we will study here the $U_\alpha = \infty$ case. The constraint of preventing double-occupancy on the dots is fulfilled by introducing two Lagrange multipliers λ_1 and λ_2. The slave boson formalism consists of writing the impurity fermionic operator on each dot as a combination of a pseudofermion and a boson operator: $d_{\sigma\alpha} = b^\dagger_\alpha f_{\sigma\alpha}$. Here $f_{\sigma\alpha}$ is the pseudofermion which annihilates one "occupied state" on dot α and $b^\dagger_\alpha$ is a bosonic operator which creates an empty state on dot α. The mean field approximation consists of replacing the bosonic operator by its expectation value: $b^\dagger_\alpha \to \left\langle b^\dagger_\alpha \right\rangle = r_\alpha$. Thus r_α and λ_α together form four parameters which need to be determined using mean field equations. Under the slave boson formalism combined with the mean field approximation, Eq. (1) reads

$$\begin{aligned} H_{SBMFT} &= -i\sum_{l\sigma}\int_{-\infty}^{+\infty} dx c^\dagger_{l\sigma}\partial_x c_{l\sigma} + \sum_{l\alpha\sigma}\tilde{V}_{l\alpha}\left(c^\dagger_{l\sigma}f_{\sigma\alpha} + \text{h.c}\right) \\ &+ \sum_{\sigma\alpha}\tilde{\epsilon}_{d\alpha}f^\dagger_{\sigma m}f_{\sigma m} + i\sum_\alpha \lambda_\alpha(r^2_\alpha - 1) \end{aligned} \tag{6}$$

with $\tilde{V}_{l\alpha} = r_\alpha V_{l\alpha}$ and $\tilde{\epsilon}_{d\alpha} = \epsilon_{d\alpha} + i\lambda_\alpha$. The mean field equations are the constraints for the dot $\alpha = 1, 2$,

$$\sum_\sigma < f^\dagger_{\alpha\sigma}(t) f_{\alpha\sigma}(t) > + r^2_\alpha = 1, \tag{7}$$

and the equation of motion (EOM) of the boson fields,

$$\text{Re}\left[\sum_{l,k,\sigma}\tilde{V}^*_{l\alpha}\left\langle c^\dagger_{kl\sigma}(t) f_{\sigma\alpha}(t)\right\rangle\right] + i\lambda_\alpha r^2_\alpha = 0. \tag{8}$$

The above equations can be understood as arising from the conditions

$$\begin{aligned} \frac{\partial\left\langle H_{SBMFT}\right\rangle}{\partial\lambda_\alpha} &= 0; \\ \frac{\partial\left\langle H_{SBMFT}\right\rangle}{\partial r_\alpha} &= 0. \end{aligned} \tag{9}$$

Thus the reality condition on Eqn. 2.8 arises from the reality of the hopping term in the Hamiltonian.[34] For any given set of bare parameters $(\epsilon_{d\alpha\sigma}, V_{l\alpha})$ we can compute the renormalized energy $(\tilde{\epsilon}_{d\alpha\sigma})$ and renormalized hybridization $(\tilde{V}_{l\alpha})$ by solving the four equations, Eqns. 7 and 8. While these results are mean field, they allow one to span a wide parameter space not constrained by the requirements of integrability. For instance, we study asymmetrically coupled dots where two channels couple to the dot, a case not solvable by the Bethe Ansatz. SBMFT allows one also, unlike the Bethe ansatz, to readily study such quantities as the spin-spin correlation function.

III. RESULTS

In this section we present a number of measures as computed using both the Bethe ansatz and slave boson mean field theory that are indicative of the ground state of the double dot plus lead system. We will argue that these are consistent with the ground state of the dot being a singlet state, not a doublet.

A. Zero Temperature Conductance

The first measure we examine is the zero temperature linear response conductance, G. For the BA, G is computed as is discussed in great detail in Refs. 31 and 12. For the SBMFT, G is computed by first solving for the variational parameters, r_α, and $\tilde{\epsilon}_{d\alpha}$, $\alpha = 1, 2$, and then determining the corresponding transmission amplitude via solving a one-particle Schrödinger equation. This procedure is detailed in Appendix B.

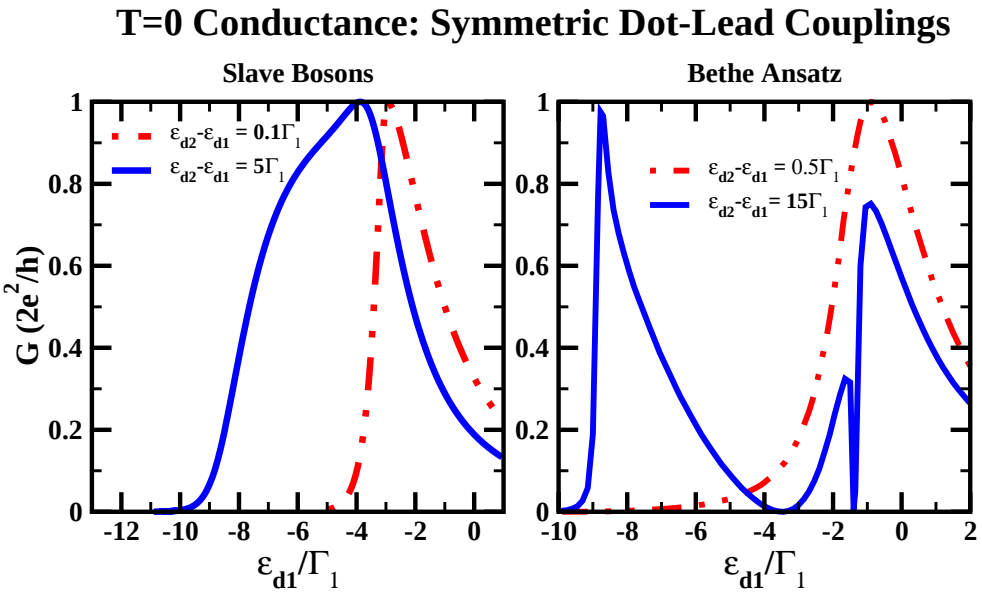

FIG. 2: The zero temperature conductance of a symmetrically coupled (i.e. one channel) double dot computed using slave boson mean field theory and the Bethe ansatz. In the case of the Bethe ansatz, the following parameters were used: $U_1 = 1$, $U_2 = 0.5$, $\Gamma_1 = U_1/30$, and $\Gamma_2 = U_1/15$. For slave bosons, we took all $V_{ij} = 1$ so that $\Gamma_1 = \Gamma_2 = 1$.

If the double dot is in a singlet state, we expect G to vanish as $\epsilon_{d1,2}$ are lowered, moving the dot into the Kondo regime. This is consistent with understanding the singlet state as a Fermi liquid state. If a Fermi liquid, G will obey the Friedel sum rule:[44]

$$G = \sum_{\sigma=\uparrow,\downarrow} \frac{e^2}{h} \sin^2(\pi n_{d\sigma}), \tag{10}$$

where $n_{d\sigma}$ is the number of electrons of spin species σ displaced by the dot. Deep in the Kondo regime, there will be two electrons sitting on the two dots, one of each spin species, i.e. $n_{d\sigma} = 1$, and so G correspondingly vanishes.

Plotted in Fig. 2 is the zero temperature conductance as computed with BA and SBMFT as a function of ϵ_{d1} and with $\epsilon_{d1} - \epsilon_{d2}$ fixed. For each computational methodology we present results for both $\epsilon_{d1} - \epsilon_{d2} \gg \Gamma_{1,2}$ and $\epsilon_{d1} - \epsilon_{d2} \ll \Gamma_{1,2}$. We see that in all cases that as $\epsilon_{d1,2}$ is lowered, the conductance vanishes.

Now that the SBMFT shows a correspondence between the number of electrons and the conductance is not suprising. Because the SBMFT always ends up treating a quadratic Hamiltonian, the Friedel sum rule necessarily holds for SBMFT. (We demonstrate this explicitly for a more general Hamiltonian involving interdot hopping in Appendix C.) However this does not necessarily imply the SBMFT could not at least mimic certain aspects of non-Fermi liquid behavior, say the conductance going to the unitary maximum, indicative of a partially screened triplet. In such a case for SBMFT the dot occupancy would then necessarily go to unity as $\epsilon_{d1,2}$ is lowered. However we find that it does not.

While the SBMFT and the BA agree on the vanishing of the conductance as $\epsilon_{d1,2}$ becomes negative, we do note that the overall structure of the conductance differs as computed between the BA and SBMFT, that is to say, the

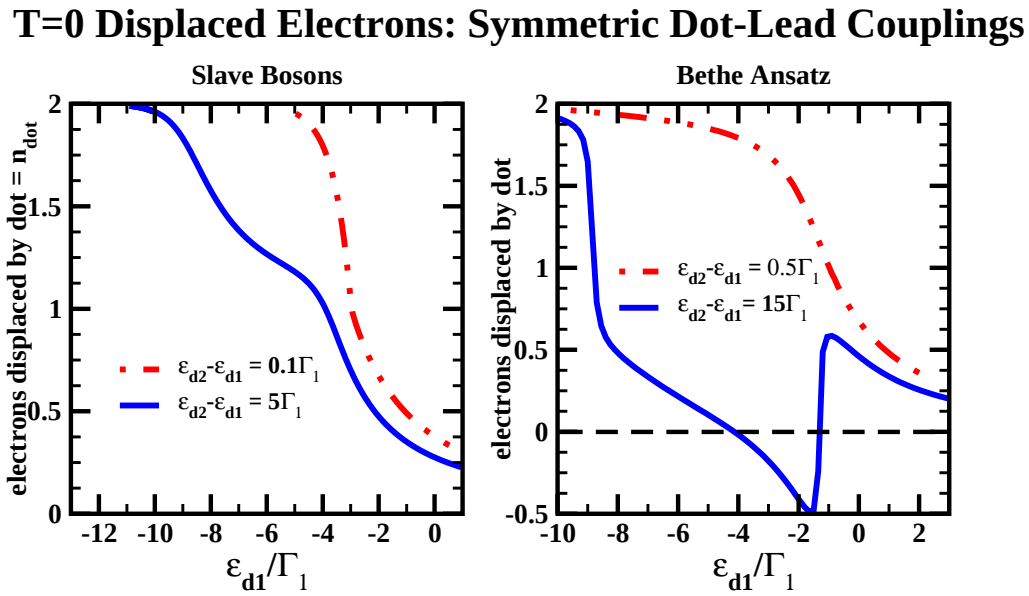

FIG. 3: The number of electrons displaced by the dots, n_d of a symmetrically coupled double dot computed both using SBMFT and the Bethe ansatz. In the case of SBMFT, n_d is simply the dot occupation, $n_{dot} = \sum_{i\sigma}\langle d^\dagger_{i\sigma} d_{i\sigma}\rangle$. In the case of the Bethe ansatz, the quantity plotted is equal to the dot occupation *plus* the $1/L$ correction to the electron density in the leads induced by coupling the dots to the leads. The parameters used for the SBMFT and Bethe ansatz computations are the same as in Fig. 2.

SBMFT fails in general to describe the correct behaviour. In particular it fails to describe the intermediate valence regime when the distance separating the chemical potential of the two dots is large, i.e $\epsilon_{d1} - \epsilon_{d2} \gg \Gamma_{1,2}$. In the intermediate valence regime the conductance of the double dot as computed with the BA undergoes rapid changes, a consequence of interference between electrons tunneling off and on the dot (see Ref. 12). This is not mirrored in the SBMFT computations which remain comparatively structureless.

The failure of SBMFT to accurately capture the physics in the intermediate valence regime is seen in a related quantity, the number of electrons displaced by the dot. n_d is the sum of two terms:

$$n_d = \sum_{\sigma i}\langle d^\dagger_{\sigma i} d_{\sigma i}\rangle + \sum_{\sigma l}\int dx \left[\langle c^\dagger_{\sigma l} c_{\sigma l}\rangle - \rho_{\sigma_{\rm bulk}}\right]. \tag{11}$$

The first term is simply the occupancy of the double dots while the second term measures the deviation of electron density in the leads due to coupling the dots and the leads. In SBMFT this term is zero due to the mean field nature of its approximation. However in BA this term is non-zero. While we cannot compute it directly, the BA gives us the ability to compute n_d. And as plotted on the r.h.s. of Fig. 3, we see that n_d can be negative. As $\sum_{\sigma i}\langle d^\dagger_{\sigma i} d_{\sigma i}\rangle$ is manifestly a positive quantity, we know that as computed by the BA, the second term in Eq.(11) is non-zero and in fact is negative (at least in the case $\epsilon_{d1} - \epsilon_{d2} \gg \Gamma_{1,2}$). From Fig. 3 we see however that n_d for both SBMFT and BA tends to two as the system enters the Kondo regime (where two electrons sit on the two dots).

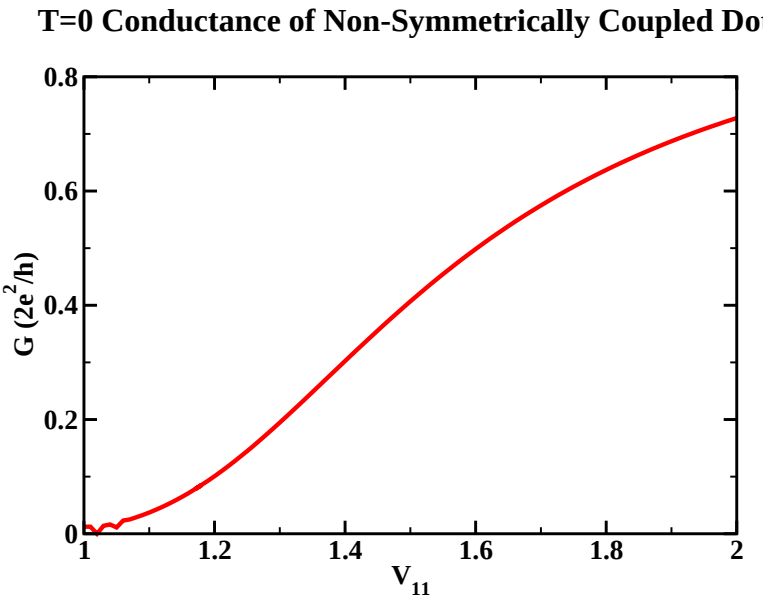

FIG. 4: The zero temperature conductance of asymmetrically coupled double dot computed using slave boson mean field theory. The conductance is plotted as a function of V_{11}. The remaining dot-lead hopping strengths are all set to 1 while $\epsilon_{d1} = -4.7$ and $\epsilon_{d2} = -4.6$. The system is in the Kondo regime, i.e. there are approximately two electrons on the two dots.

One advantage the SBMFT does offer over the BA is that it allows us to compute transport quantities beyond the integrable parameter regime delineated in Eq. (2). It was argued in Ref.12 that small deviations away from this parameter space should not qualitatively change transport properties. In Fig. 4 we test this in the Kondo regime (where we expect SBMFT to be at its most accurate) computing the conductance while adjusting the dot-lead hopping parameters in such a way that we move from a case where only one effective channel couples to the quantum dot (i.e. $V_{ij} = 1$) to a case where two channels couple to the dot ($V_{11} > 1$ and $V_{12} = V_{21} = V_{22} = 1$). We see when the second channel is only weakly coupled to the dot, the conductance remains near its one-channel value, i.e. $G = 0e^2/h$. Only once V_{11} appreciably deviates from 1 do we see a corresponding deviation in G. We note that this continuous behaviour is also consistent with the one-channel dot-lead ground state being a singlet. If it were instead a doublet, coupling a second channel into the system would lead to a discontinuous change as the second channel, no matter how weakly coupled, would immediately screen the free effective spin-1/2.

Finally in this section we consider the behaviour of the conductance and displaced electrons when $\epsilon_{d1} = \epsilon_{d2}$. We see from Fig. 5 that the same qualitative behaviour in both quantities is found using the Bethe ansatz and using SBMFT. Namely, the displaced electron number n_d tends to 2 while the conductance G tends to zero as $\epsilon_{d1} = \epsilon_{d2}$ goes to zero. While these measures are the same in the two computational methods, there is a quantity that sharply distinguishes the two (and so shows a failure of SBMFT even in the Kondo regime at zero temperature). This quantity is the low lying density of states on the dots, $\rho_d(\omega)$. For the case of $\epsilon_{d1} = \epsilon_{d2}$, the BA shows that $\rho_d(\omega)$ for ω on the order of the Kondo temperature, T_K vanishes.[12] However the SBMFT shows that at this energy scale there exists non-negligible spectral weight. In Fig. 6, we plot $\rho_d(\omega)$ as defined by

$$\rho_d(\omega) = \sum_{i\sigma} \mathrm{Im}\langle d^\dagger_{i\sigma} d_{i\sigma}\rangle_{retarded}.$$

The agreement on the qualitative features of n_d and G between the two methodologies is then a coincidence (to a degree). In both cases the ground state is Fermi liquid like and so G follows the Friedel sum rule which necessarily mandates that the conductance vanish with two electrons on the two dots. But the nature of the Fermi liquid in each case as predicted by the methodologies is much different. SBMFT predicts the scale of the low lying excitations is T_K while the BA finds that for the special case of $\epsilon_{d1} = \epsilon_{d2}$ (and only for this case[12]) that the fundamental energy scale corresponds to the bare energies scales in the problem, i.e. U and Γ.

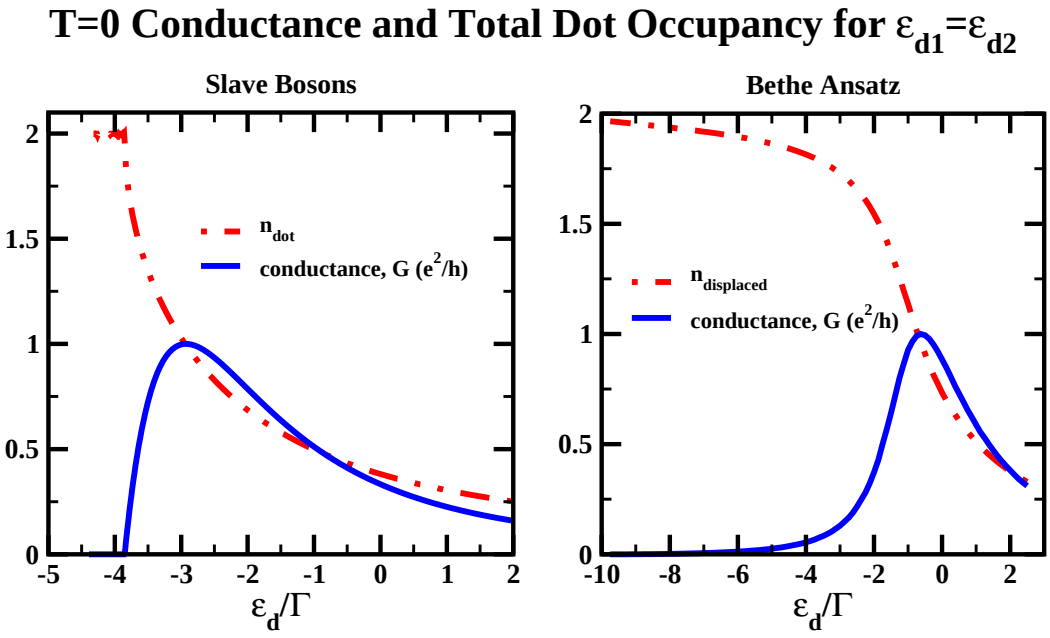

FIG. 5: The conductance and the number of displaced electrons as a function of $\epsilon_{d1}(=\epsilon_{d2})$ as computed using SBMFT and the Bethe ansatz. For the Bethe ansatz we choose as parameters $U = U1 = 0.8$ and $\Gamma_1 = \Gamma_2 = 0.04$. For slave bosons we take all $V_{ij} = 1$ (and so $\Gamma_{1,2} = 1$).

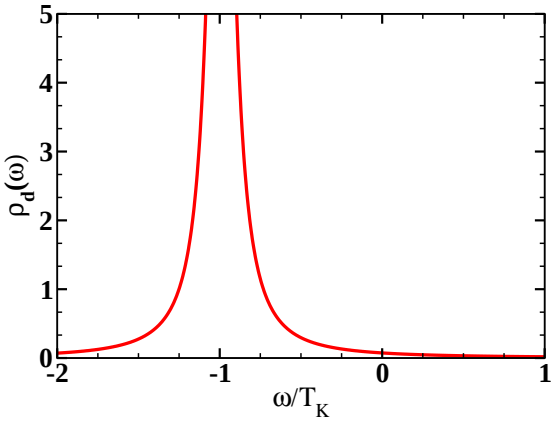

FIG. 6: A plot of the low energy density of states, $\rho(\omega)$ for $\epsilon_{d1} = \epsilon_{d2} = -4.45\Gamma_{1,2}$ in the Kondo regime as computed using SBMFT. (We again take $\Gamma_{1,2} = 1$ here.) As we are argue in the text, this is an artifact of SBMFT (the BA shows that in this case $\rho_d(\omega)$ vanishes[12]).

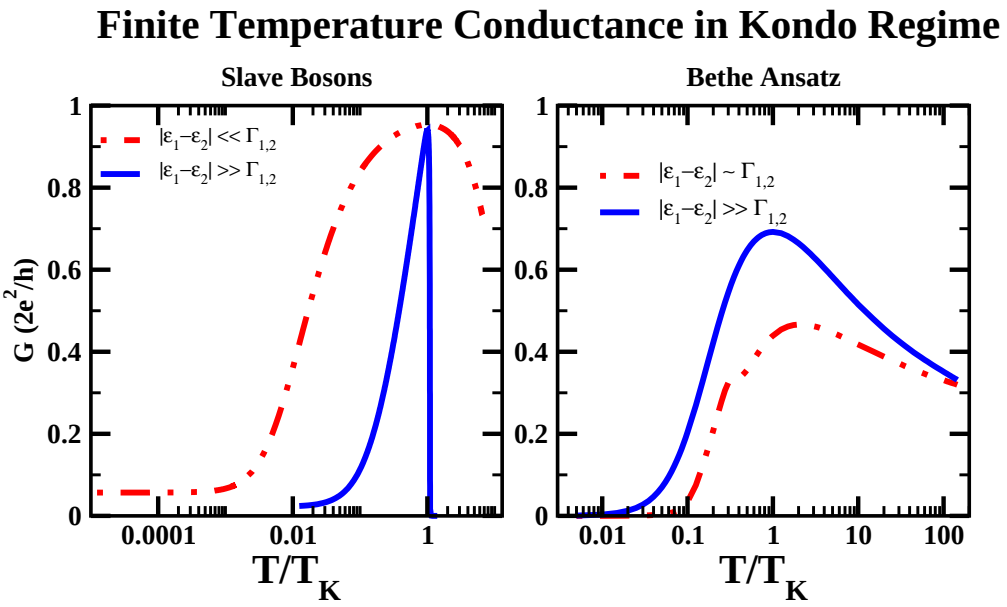

FIG. 7: The linear response conductance as a function of temperature of a symmetrically coupled double dot computed using both slave boson mean field theory and the Bethe ansatz. For the case of small separation in the slave boson approach, we set $\Gamma_{1,2} = 1$ and took $\epsilon_1 - \epsilon_2 = 0.05$ and $\epsilon_1 = -4.1$. For the large separation case, we correspondingly took $\epsilon_1 - \epsilon_2 = 5$ and $\epsilon_1 = -9.4$. In the Bethe ansatz computations, we took in the case $|\epsilon_1 - \epsilon_2| \sim \Gamma_{1,2}$, $U_1 = 1$, $\Gamma_1 = 0.05$, $U_2 = 0.9$, $\Gamma_2 = 1/18$, $\epsilon_1 = -0.5$ and $\epsilon_2 = -0.45$. For the case $|\epsilon_1 - \epsilon_2| >> \Gamma_{1,2}$, $U_1 = 1$, $\Gamma_1 = 0.05$, $U_2 = 0.4$, $\Gamma_2 = 0.125$, $\epsilon_1 = -0.5$ and $\epsilon_2 = -0.2$.

B. Finite Temperature Conductance

We now consider the finite temperature conductance. Plotted in Fig. 7 are traces for $G(T)$ for double dots with both $|\epsilon_{d1} - \epsilon_{d2}| \gg \Gamma_{1,2}$ and $|\epsilon_{d1} - \epsilon_{d2}| \ll \Gamma_{1,2}$ as computed with both the Bethe ansatz as well as SBMFT. For a Fermi liquid ground state we expect that at low temperatures the conductance deviate from its zero temperature value by T^2 and we see that behaviour in both cases. From Fig. 7 we see that in both treatments, the finite temperature conductance for the double dots initial rises with increasing temperature to an appreciable fraction of the unitary maximum and thereafter decreases in an uniform manner (regardless of the bare level separation). (For SBMFT we have defined the Kondo temperature as where this peak in $G(T)$ occurs while for the BA the Kondo temperature we employ the analytic expression for T_K of the double dots derived in Ref. 12.) We however also see that there are qualitative differences between SBMFT and the Bethe ansatz. The peak in the conductance computed using SBMFT peaks at a value far closer to the unitary maximum than does the Bethe ansatz. And we also see that the conductance as computed in the SBMFT drops off far more rapidly than it does in the BA (particularly at large level separation). We however believe this is unphysical and akin to the pathologies that SBMFT is known to exhibit at higher temperatures and energy scales.[34–40]

As was demonstrated in Ref. 12, the conductance at finite but small T is quadratic in T while at large T the conductance is logarithmic (going as $1/\log^2(T/T_K)$). The peak in conductance at finite T is then a result of the conductance vanishing in the low and high temperature limits. These conductance profiles are similar to the those

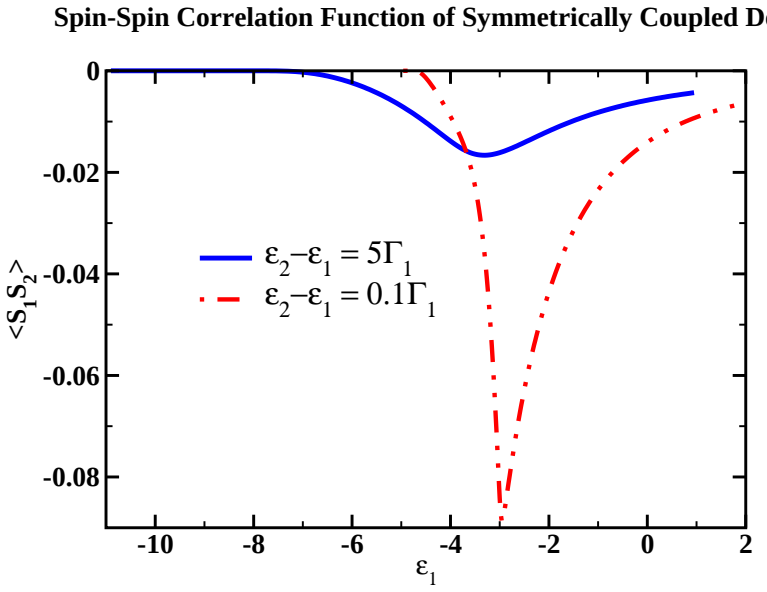

FIG. 8: The spin-spin correlation function of symmetrically coupled double dot computed using slave boson mean field theory. We again take $V_{ij} = 1$.

predicted in Ref. 41 for multi-dots coupled to *two* electron channels. However the physics there is much different: the non-monotonicity in $G(T)$ predicted in Ref. 41 is due to the presence of the two channels and because they couple to the dots with different strengths, they screen a $S > 1/2$ state in stages.

C. Spin-Spin Correlation Function

We present the static spin-spin correlation function as a function of ϵ_{d1} and as computed using SBMFT in Fig. 8. With two electrons on the dot the value of $\langle S_1 \cdot S_2 \rangle$ can vary between $-3/4$ (if these two electrons are bound in a singlet state) to $1/4$ (if the two electrons find themselves in a triplet state). We see in Fig. 8 that generically the value of the correlation function in the Kondo regime (for the relevant values of ϵ_{d1} see Fig. 2) that $\langle S_1 \cdot S_2 \rangle$ tends to 0. This however should not necessarily be interpreted as the dots being closer to a triplet state than a singlet state. In determining the overall state of the system, $\langle S_1 \cdot S_2 \rangle$, is not necessarily a good measure. We can see this by considering a simple toy example.

Imagine a system of four spins, two associated with the dots, $|\uparrow\rangle_{d1}$ and $|\uparrow\rangle_{d2}$, and two associated with leads $|\uparrow\rangle_{l1}$ and $|\uparrow\rangle_{l2}$. And first suppose the system is in a singlet state. Two ways this singlet state can be formed are

$$\begin{aligned} |\text{singlet 1}\rangle &= \frac{1}{2}(|\uparrow\rangle_{d1}|\downarrow\rangle_{d2} - |\downarrow\rangle_{d1}|\uparrow\rangle_{d2}) \otimes (|\uparrow\rangle_{l1}|\downarrow\rangle_{l2} - |\downarrow\rangle_{l1}|\uparrow\rangle_{l2}); \\ |\text{singlet 2}\rangle &= \frac{1}{2}(|\uparrow\rangle_{l1}|\downarrow\rangle_{d1} - |\downarrow\rangle_{l1}|\uparrow\rangle_{d1}) \otimes (|\uparrow\rangle_{l2}|\downarrow\rangle_{d2} - |\downarrow\rangle_{l2}|\uparrow\rangle_{d2}). \end{aligned} \tag{12}$$

We see that the expectation value, $\langle S_1 \cdot S_2 \rangle$, of these two states is considerably different:

$$\begin{aligned} \langle \text{singlet 1}|S_1 \cdot S_2|\text{singlet 1}\rangle &= -3/4 \\ \langle \text{singlet 2}|S_1 \cdot S_2|\text{singlet 2}\rangle &= 0. \end{aligned} \tag{13}$$

Now suppose the system is in a triplet state and suppose its S_z projection is 1. Again there are two inequivalent ways this state can be formed:

$$|\text{triplet 1}\rangle = \frac{1}{\sqrt{2}}|\uparrow\rangle_{d1}|\uparrow\rangle_{d2} \otimes (|\uparrow\rangle_{l1}|\downarrow\rangle_{l2} - |\downarrow\rangle_{l1}|\uparrow\rangle_{l2});$$

$$|\text{triplet } 2\rangle \;=\; \frac{1}{\sqrt{2}}|\uparrow\rangle_{l1}|\uparrow\rangle_{d1}\otimes(|\uparrow\rangle_{l2}|\downarrow\rangle_{d2}-|\downarrow\rangle_{l2}|\uparrow\rangle_{d2}). \tag{14}$$

The expectation of these two values is

$$\begin{aligned}\langle\text{triplet } 1|S_1\cdot S_2|\text{triplet } 1\rangle \;&=\; 1/4\\ \langle\text{triplet } 2|S_1\cdot S_2|\text{triplet } 2\rangle \;&=\; 0.\end{aligned} \tag{15}$$

We thus see that when the system's state is such that $\langle S_1\cdot S_2\rangle = 0$, it can be either a singlet or a triplet equally. We thus end with a more reliable measure of the dot's internal degrees of freedom: the impurity entropy.

D. Impurity Entropy

The final set of computations we present in this section are of the impurity entropy of the double dots with two electrons on the dots. In Fig. 9 we plot results coming from SBMFT and the BA for both large and small level separation. (The derivation of the impurity entropy in the context of the BA is found in Appendix A.) We see that in all cases the impurity entropy vanishes as $T\to 0$. This then implies the ground state of the double dot system is a singlet. If it were a triplet state, the $T\to 0$ limit would lead to $S_{imp}=\log(2)$.

IV. DISCUSSION AND CONCLUSIONS

We have presented a number of arguments that the ground state of a double dot near the particle-hole symmetric point (i.e. when there are nearly two electrons on the dots) is in a singlet Fermi liquid state. In particular we have shown that the conductance in this limit vanishes, in accordance with the Friedel sum rule and that the impurity entropy also vanishes, in agreement with the ground state being a singlet.

These conclusions however disagree with a number of NRG studies. In Refs. 13 and 14 it is found that a double quantum dot (with the dots closely spaced) carrying two electrons is in a spin-triplet state, has a conductance corresponding to the unitary maximum, and is correspondingly a non-Fermi liquid. Similar conclusions are reached in Refs. 16,17. The basic rational invoked for observing this physics is that with dots closely spaced, a ferromagnetic RKKY interaction is present which binds the two electrons on the dot into a spin triplet. Consequently the ground state of the double dot is that of an underscreened spin-1 Kondo impurity.

This intuition is very appealing. But it is not free from criticism. This argument is most compelling at temperatures above any putative Kondo temperature. The perturbation theory underlying the RKKY interaction becomes uncontrolled as temperature is lowered below any Kondo temperature. Below such a temperature, one might expect (because of the presence of Kondo physics) to at least perform a summation of leading logs at all orders in the perturbation theory in order to ascertain the nature of any RKKY interaction. This point, in essence, has been made by Fye, when he questions whether the zero temperature perturbation theory underlying any RKKY estimate is convergent because the system is gapless.[45]

This intuition also treats the two electrons sitting on the two dots as a non-composite spin-1 object (at least at sufficiently low temperatures). However allowing the electrons to maintain their distinctness suggests another screening scenario. Focusing on one of the two electrons, one can imagine a situation where the electron is screened by a combination of the other localized electron together with the conduction electrons, i.e. the screening channel is composed of two pieces. This interpretation would be one way to reconcile the Bethe ansatz/SBMFT results with the simpler intuition that a screening channel is only able to screen spin-1/2.

Beyond questioning whether a ferromagnetic RKKY interaction does indeed form between two closely spaced dots and temperatures lower than the Kondo temperature, we offer two possible reasons for the discrepancy that we find between the Bethe ansatz/SBMFT and the NRG studies. The first possibility is that the Bethe ansatz and SBMFT solutions of the double dots are treating the short distance physics in the problem in a different fashion than the NRG studies. It may well be that the physics of the double dots is sensitive to how the high energy sector is modelled. It is not unnatural to think this may be the case as the physics depends on how two closely spaced dots interact with one another. And certainly the methodologies have different UV cutoffs. Both the Bethe ansatz and SBMFT assume a linearly dispersing spectrum of conduction electrons that is cutoff beyond a fixed energy. The NRG, on the other hand, maps a continuum Fermi sea of electrons to a set of electrons living on an infinite half line lattice which is then studied through a numerically optimized matrix product ansatz wavefunction. It thus seems unlikely that the effective UV cutoff in the NRG is the same as that of the Bethe ansatz/SBMFT.

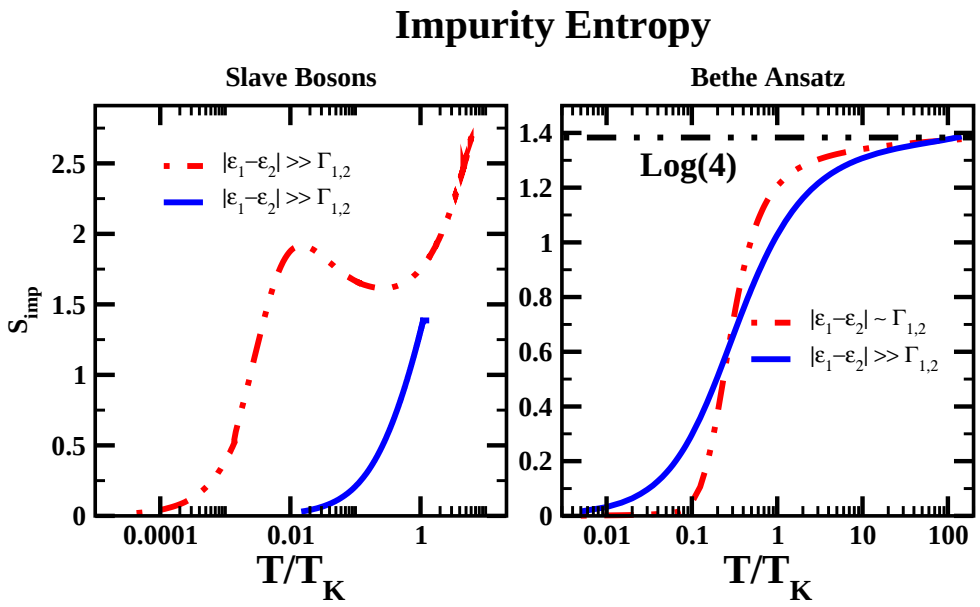

FIG. 9: The impurity entropy as a function of temperature of a symmetrically coupled double dot computed using slave boson mean field theory and the Bethe ansatz. For the slave boson computations, we use the same parameters as found in Fig. 7. For the Bethe ansatz computations, we took in the case $|\epsilon_1 - \epsilon_2| \sim \Gamma_{1,2}$, $U_1 = 1$, $\Gamma_1 = 0.05$, $U_2 = 0.95$, $\Gamma_2 = 1/19$, $\epsilon_1 = -0.5$ and $\epsilon_2 = -0.475$. For the case $|\epsilon_1 - \epsilon_2| >> \Gamma_{1,2}$, we used $U_1 = 1$, $\Gamma_1 = 0.05$, $U_2 = 0.5$, $\Gamma_2 = 0.10$, $\epsilon_1 = -0.5$ and $\epsilon_2 = -0.25$.

Another possibility that we offer as a suggestion for the discrepancy is in the nature of the approximation the NRG makes in treating the double dot problem. In solving this problem, the NRG discards a number of degrees of freedom coming the continuum set of electrons. In the single dot case, it is known[49] that these degrees of freedom are unimportant, even on a quantitative level, for describing the physics. But it is unclear (at least to us) if this is universally so or whether these degrees of freedom matter for more complicated dots systems. We will describe a possible scenario of how these degrees of freedom might matter. We emphasize, however, that this is only a conjecture. A real test would involve actually taking into account these degrees of freedom in the NRG algorithm and seeing if there is any real difference.

The Anderson Hamiltonian typically considered in these studies is of the form:

$$\begin{aligned} H &= H_{lead} + H_{dot} + H_{lead-dot}; \\ H_{lead} &= D\int_{-1}^{1} kdk a^{\dagger}_{k\sigma} a_{k\sigma}; \\ H_{dot} &= \sum_{i=1,2;\sigma} \epsilon_{di} d^{\dagger}_{i\sigma} d_{i\sigma} + \sum_i U_i n_{i\uparrow} n_{i\downarrow}; \\ H_{dot-lead} &= D^{1/2} \sum_{i\sigma} \int_{-1}^{1} dk\ V_i (d^{\dagger}_{i\sigma} a_{k\sigma} + a^{\dagger}_{k\sigma} d_{i\sigma}) \end{aligned} \tag{16}$$

where we are using the conventions of Ref. 48 in writing down the NRG Hamiltonian. Before implementing the NRG algorithm, one adopts a logarithmic basis for the lead electrons,

$$a_{k\sigma} \;=\; \sum_{np} a_{np\sigma}\psi^{+}_{np}(k) + b_{np\sigma}\psi^{-}_{np}(k), \tag{17}$$

where

$$\psi^{\pm}_{np}(k) = \begin{cases} \frac{\Lambda^{n/2}}{(1-\Lambda^{-1})^{1/2}} e^{\pm i\omega_n pk} & \text{if } \Lambda^{-(n+1)} < \pm k < \Lambda^{-n}, \\ 0 & \text{if k is not within the above interval,} \end{cases} \tag{18}$$

and w_n is given by

$$w_n = \frac{2\pi\Lambda^n}{1-\Lambda^{-1}}. \tag{19}$$

Here Λ is a parameter less than one. This change of basis transforms H_{lead} and $H_{lead-dot}$ into

$$\begin{aligned} H_{lead} \;&=\; \frac{D}{2}(1+\Lambda^{-1})\sum_{np}\Lambda^{-n}(a^{\dagger}_{np\sigma}a_{np\sigma} - b^{\dagger}_{np\sigma}b_{np\sigma}) \\ &\quad + \frac{D(1-\Lambda^{-1})}{2\pi i}\sum_{n}\sum_{p\neq p'}\exp(\frac{2\pi i(p'-p)}{1-\Lambda^{-1}})(a^{\dagger}_{np\sigma}a_{np'\sigma} - b^{\dagger}_{np\sigma}b_{np'\sigma})\frac{\Lambda^{-n}}{p'-p}; \\ H_{lead-dot} \;&=\; D^{1/2}(1-\Lambda^{-1})^{1/2}\sum_{in\sigma}\Lambda^{-n/2}V_i((a^{\dagger}_{n0\sigma} + b^{\dagger}_{n0\sigma})d_i + \text{h.c.}). \end{aligned} \tag{20}$$

Typically the approximation that is now made in most NRG treatments (and seems to have been made in the above references) is that the $p \neq 0$ modes of the logarithmic basis are dropped, not least because these modes do not directly couple to dot. As stated, in the single dot case, where this approximation was first made,[48,49] this was found to be a (more than) reasonable approximation. However in the double dot case it is not *a priori* obvious that this is the case. In particular if one finds an underscreened Kondo effect one might ask whether that additional modes ($p \neq 0$) might serve to provide additional screening.

Let us then consider the NRG Hamiltonian that would arise if both the $p = 0$ and $p = \pm 1$ modes were kept. H_{lead} can then be trivially diagonalized using the combination

$$\begin{aligned} r_{n0\sigma} \;&=\; \frac{1}{3}\left(2a_{n1\sigma} - e^{\theta}a_{n0\sigma} + 2e^{2\theta}a_{n-1\sigma}\right); \\ r_{n\pm\sigma} \;&=\; \frac{1}{3\sqrt{10}}\left[5a_{n1\sigma} + (2\mp 6i)e^{\theta}a_{n0\sigma} - (4\pm 3i)e^{2\theta}a_{n-1\sigma}\right], \end{aligned} \tag{21}$$

with $\theta = -\frac{2\pi i}{1-\Lambda^{-1}}$. Note that the corresponding transformation $\{s \leftrightarrow b\}$ is omitted for brevity. This yields

$$\begin{aligned} H_{lead} \;&=\; D\sum_{n\sigma}\Lambda^{-n}\Bigg\{\frac{1+\Lambda^{-1}}{2}r^{\dagger}_{n0\sigma}r_{n0\sigma} + \frac{2\pi(1+\Lambda)+3(1-\Lambda)}{4\pi\Lambda}r^{\dagger}_{n+\sigma}r_{n+\sigma} \\ &\quad + \frac{2\pi(1+\Lambda)-3(1-\Lambda)}{4\pi\Lambda}r^{\dagger}_{n-\sigma}r_{n-\sigma} - \{r\to s\}\Bigg\} \end{aligned} \tag{22}$$

The corresponding transformation of dot-lead Hamiltonian is

$$H_{dot-lead} = \sum_{in\sigma}V_{ni}\left[\sqrt{\frac{2}{5}}\left(\frac{1}{3}-i\right)r^{\dagger}_{n+\sigma}d_{i\sigma} + \sqrt{\frac{2}{5}}\left(\frac{1}{3}+i\right)r^{\dagger}_{n-\sigma}d_{i\sigma} - \frac{1}{3}r^{\dagger}_{n0\sigma}d_{i\sigma} + \{r\to s\} + h.c\right], \tag{23}$$

with $V_{ni} = D^{\frac{1}{2}}(1-\Lambda^{-1})^{\frac{1}{2}}\Lambda^{-\frac{n}{2}}e^{\theta}V_i$.

We see upon this diagonalization that three channels of electrons, $r_{n\{0,\pm\},\sigma}$ and $s_{n\{0,\pm\}\sigma}$, couple to the dot. And because of the nature of the logarithmic basis, we see that $+$, $-$ and 0 variables can be arbitrarily close to the Fermi surface (due to the presence of the Λ^{-n} factor) we might expect all to contribute to Kondo screening.

At this point, this analysis suggests that in a situation with two electrons on the double dots which are bound into a triplet by a putative RKKY coupling, there are nonetheless (at least) three available screening channels, at least in

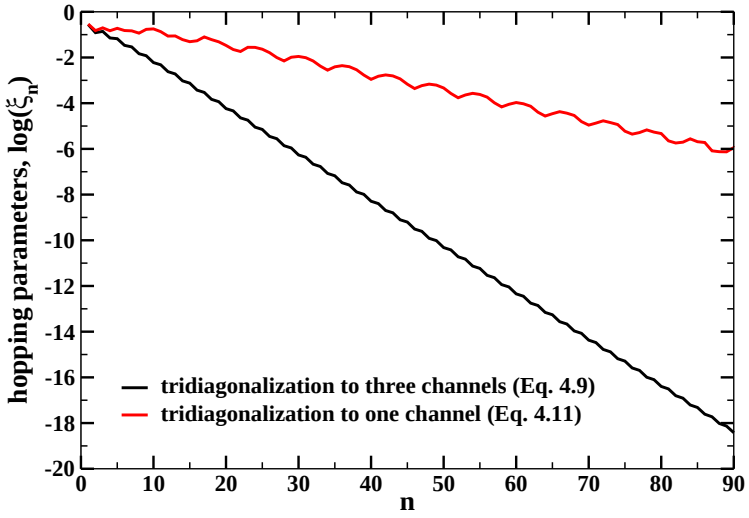

FIG. 10: Plot of the logarithmic decay of the hopping parameters in the two different tridiagonalization schemes. We see in the scheme leaving us with three channels, the hopping parameters decay with a power law exponent three times that of the tridiagonalization leaving us with one channel. In making this plot, Λ was set to 1.5.

the NRG reduction of the Anderson Hamiltonian. And so the problem would seem to be not one of an underscreened Kondo effect but of a channel-anisotropic overscreened Kondo effect.

We however note a caveat with this conclusion. The next step in the NRG analysis is to map the above Hamiltonian onto a half line lattice through a Lanczos tridiagonalization procedure. But this can be done, in fact, in two ways. We can perform a tridiagonalization on each channel $(r_\pm, r_0)$ individually. If we do so the above Hamiltonian is transformed as follows:

$$H_{lead} = \frac{D}{2}(1+\Lambda^{-1}) \sum_{n=0;\alpha=0,\pm;\sigma} \xi_{n\alpha} \left[f^\dagger_{n\alpha\sigma} f_{n+1\alpha\sigma} + f^\dagger_{n+1\alpha\sigma} f_{n\alpha\sigma} \right], \tag{24}$$

where $\xi_{n\alpha}$ are given by

$$\begin{aligned} \xi_{n0} &= \xi_n; \quad \xi_{n+} = (1+3\frac{(1-\Lambda)}{2\pi(1+\Lambda)})\xi_n; \quad \xi_{n-} = (1-3\frac{(1-\Lambda)}{2\pi(1+\Lambda)})\xi_n; \\ \xi_n &= \Lambda^{-n/2}(1-\Lambda^{-n-1})(1-\Lambda^{-2n-1})^{-1/2}(1-\Lambda^{-2n-3})^{-1/2}. \end{aligned}$$

Here the operators $f^\dagger_{n=0;\alpha=\pm,0;\sigma}$, i.e. the operators creating a conduction electron on the site next to the impurity, are defined to be

$$f^\dagger_{n=0,\sigma\alpha=0,\pm} = (\frac{1-\Lambda^{-1}}{2})^{1/2} \sum_{m=0}^{\infty} \Lambda^{-m/2}(r^\dagger_{m\alpha\sigma} + s^\dagger_{m\alpha\sigma}). \tag{25}$$

In this way we obtain what could be described as a channel-anisotropic overscreened Kondo effect.

But we can in fact also perform the tridiagonalization on all three sets of modes simultaneously, leaving us with a lead Hamiltonian of the form

$$H_{lead} = \frac{D}{2}(1+\Lambda^{-1}) \sum_{n=0\sigma} \tilde{\xi}_n \left[\tilde{f}^\dagger_{n\alpha\sigma} \tilde{f}_{n+1\alpha\sigma} + \tilde{f}^\dagger_{n+1\alpha\sigma} \tilde{f}_{n\alpha\sigma} \right]. \tag{26}$$

where the operator $\tilde{f}^\dagger_{m=0}$ is now defined as

$$\tilde{f}^\dagger_{m=0\sigma} \propto \sum_n \left[\sqrt{\frac{2}{5}} \left(\frac{1}{3} - i \right) (r^\dagger_{n+\sigma} + s^\dagger_{n+\sigma}) + \sqrt{\frac{2}{5}} \left(\frac{1}{3} + i \right) (r^\dagger_{n-\sigma} + s^\dagger_{n-\sigma}) - \frac{1}{3}(r^\dagger_{n0\sigma} + s^\dagger_{n0\sigma}) \right]. \tag{27}$$

If we were to reexpress $\tilde{f}_n$ in terms of $f_{ni=\pm,0}$, we would find that $\tilde{f}_n$ are not simple linear combinations of $f_{ni=\pm,0}$ for the same n but rather involve $f_{ni=\pm,0}$ for all n. That is, the two tridiagonalizations are not locally related to one another. It raises then the question of how to determine how many effective channels are coupled to the impurity degrees of freedom. At the very least, the two different tridiagonalizations suggest two different answers.

One observation we do make is that in the two lattice models arrived at by the two tridiagonalizations, the effective hopping parameters fall off with different power laws. In the tridiagonalization yielding three channels, the hopping parameters $\xi_{n,i=\pm,0}$ fall off as $\Lambda^{-n/2}$. In the second tridiagonalization the hopping parameters, $\tilde{\xi}_n$ appear to fall (at least numerically) as $\Lambda^{-n/6}$. Thus we see at least that the two tridiagonalizations contain (roughly speaking) the same number of degrees of freedom. In the first case we have a three channel model falling off as $\Lambda^{-n/2}$, while in the second case we have a one channel model that appears, because of the slower decay of the hopping parameters, to have a unit cell with a basis size of three.

While we draw no definitive conclusions from this discussion of the mechanics of the NRG, we believe we have at least raised both the question of whether the $p \neq 0$ modes play a role in determining the physics of the double dots as well as the question of whether the results of the NRG are clearly independent of the details of the particular choice of tridiagonalization.

Acknowledgements: MK was supported by the NSF under grant no. DMR-0906866. RMK acknowledges support by the US DOE under contract number DE-AC02-98 CH 10886. We thank Rok Zitko, Chung-Hou Chung, Alexei Tsvelik, Piers Coleman and Leonid Glazman.

Appendix A: Analysis of the Ground State Entropy via the TBA Equations

Here it is demonstrated that the ground state entropy of the double dot system at zero temperature is zero and thus the ground state is a singlet. The procedure outlined below can be found for a single dot in Section 8.3.3 of Ref. 42.

We start with the observation that the free energy of the system can be expressed as sums over all excitations in the system, that is, over all possible solutions of the Bethe ansatz equations (see Eqn. 10 of Ref. 12). Specifically it takes the form

$$\Omega \;=\; E - TS, \tag{A1}$$

where the energy of the system equals

$$E \;=\; \int dk \rho(k) k + \sum_{n=1}^{\infty} \int d\lambda \sigma_n'(\lambda) \epsilon_{0n}(\lambda), \tag{A2}$$

where

$$\begin{aligned} \epsilon_{0n}(\lambda) \;&=\; -n(2\epsilon_{d1} + U_1/2) + 2\int_{-\infty}^{\infty} a_n(\lambda - g(k)) g(k); \\ a_n(x) \;&=\; \frac{2}{\pi} \frac{1}{n^2 + 4x^2}; \\ g(k) \;&=\; \frac{(k - \epsilon_{d1} - \frac{U_1}{2})^2}{2U_1\Gamma_1}, \end{aligned} \tag{A3}$$

and the entropy, S, is given by

$$\begin{aligned} S \;=\; &\int dk \Big[(\rho(k) + \tilde{\rho}(k)) \log(\rho(k) + \tilde{\rho}(k)) - \rho(k) \log \rho(k) - \tilde{\rho}(k) \log(\rho(k)) \Big] \\ &+ \sum_{n=0}^{\infty} \Big[(\sigma_n(\lambda) + \tilde{\sigma}_n(\lambda)) \log(\sigma_n(\lambda) + \tilde{\sigma}_n(\lambda)) - \sigma_n(\lambda) \log \sigma_n(\lambda) - \tilde{\sigma}_n(\lambda) \log(\sigma_n(\lambda)) \Big] \\ &+ \sum_{n=0}^{\infty} \Big[(\sigma_n'(\lambda) + \tilde{\sigma}_n'(\lambda)) \log(\sigma_n'(\lambda) + \tilde{\sigma}_n'(\lambda)) - \sigma_n(\lambda) \log \sigma_n'(\lambda) - \tilde{\sigma}_n'(\lambda) \log(\sigma_n'(\lambda)) \Big]. \end{aligned} \tag{A4}$$

Here $\rho(k), \sigma_n(\lambda)$, and $\sigma'_n(\lambda)$ are the particle densities while $\tilde{\rho}(k), \tilde{\sigma}_n(\lambda)$, and $\tilde{\sigma}'_n(\lambda)$ are the hole densities of the various excitations (i.e. solutions of the Bethe ansatz equations). The particle and hole densities can be shown to obey the following equations:

$$\tilde{\rho}(k) + \rho(k) \;=\; \rho_0(k) - g'(k) \int d\lambda s(\lambda - g(k))(\tilde{\sigma}_1(\lambda) + \tilde{\sigma}'_1(\lambda)), \tag{A5}$$

where

$$\begin{aligned}
\rho_0(k) &= \frac{1}{2\pi} + \frac{1}{L}\Delta(k) + g'(k) \int d\lambda s(\lambda - g(k))(-\frac{1}{2\pi}\epsilon'_{01}(\lambda) + \frac{1}{L}\tilde{\Delta}_1(\lambda)); \\
\Delta(k) &= \frac{1}{2\pi}\partial_k \delta(k); \\
\tilde{\Delta}_n(\lambda) &= -\frac{1}{\pi} Re\Delta(\sqrt{2U_1\Gamma_1}(\lambda + \frac{in}{2})); \\
s(x) &= \frac{1}{2\cosh(\pi x)},
\end{aligned} \tag{A6}$$

and

$$\begin{aligned}
\tilde{\sigma}_n(\lambda) + \sigma_n(\lambda) &= \int d\lambda' s(\lambda - \lambda'))(\tilde{\sigma}_{n+1}(\lambda') + \tilde{\sigma}_{n-1}(\lambda')) + \delta_{n1} \int dk \rho(k) s(\lambda - g(k)); \\
\tilde{\sigma}'_n(\lambda) + \sigma'_n(\lambda) &= \int d\lambda' s(\lambda - \lambda'))(\tilde{\sigma}'_{n+1}(\lambda') + \tilde{\sigma}'_{n-1}(\lambda')) + D_n(\lambda),
\end{aligned} \tag{A7}$$

where

$$D_n(\lambda) \;=\; \delta_{n1} \int dk \rho(k) s(\lambda - g(k)) - \int d\lambda' s(\lambda - \lambda'))(\tilde{\Delta}_{n+1}(\lambda') + \tilde{\Delta}_{n-1}(\lambda')); \tag{A8}$$

One sees that the density equations have source terms that involve a bulk piece and a piece scaling as $1/L$, where L is the system size.

One defines the energies of the excitations at finite temperature via the relations,

$$\epsilon(k) = T\log(\frac{\tilde{\rho}(k)}{\rho(k)}); \quad \epsilon_n(\lambda) = T\log(\frac{\tilde{\sigma}_n(\lambda)}{\sigma_n(\lambda)}); \quad \epsilon'_n(\lambda) = T\log(\frac{\tilde{\sigma}'_n(\lambda)}{\sigma'_n(\lambda)}). \tag{A9}$$

These energies are given by the relations $\epsilon(k), \epsilon_n(\lambda)$, and $\epsilon'_n(\lambda)$ which are governed by the equations,

$$\begin{aligned}
\epsilon(k) &= k + \int d\lambda \epsilon_{01}(\lambda) s(\lambda - g(k)) + T \int d\lambda s(\lambda - g(k)) \log\left(\frac{n(\epsilon_1(\lambda))}{n(\epsilon'_1(\lambda))}\right); \\
\epsilon_n(\lambda) &= \delta_{n1} T \int dk g'(k) s(\lambda - g(k)) \log(n(-\epsilon(k))) \\
&\qquad -T \int d\lambda' s(\lambda - \lambda') \log(n(\epsilon'_{n-1}(\lambda)) n(\epsilon'_{n+1}(\lambda))); \\
\epsilon'_n(\lambda) &= \delta_{n1} T \int dk g'(k) s(\lambda - g(k)) \log(n(\epsilon(k))) \\
&\qquad -T \int d\lambda' s(\lambda - \lambda') \log(n(\epsilon'_{n-1}(\lambda)) n(\epsilon'_{n+1}(\lambda))),
\end{aligned} \tag{A10}$$

where $n(x) = (1 + \exp(x/T))^{-1}$ is the Fermi function. The equations for the ϵ's and the bulk pieces of the densities (i.e. the pieces not scaling as $1/L$) are the same as for a single level dot. As noted in the manuscript, the Bethe ansatz equations for the double dots in parallel are identical to the single level dot up to the impurity scattering phase.

Substituting the energies and densities in the expression for the free energy, one can rewrite it in a much more simple fashion:

$$\Omega \;=\; E_{gs} + T \int dk \rho_0(k) \log(n(-\epsilon(k))) + T \int d\lambda \sum_{n=0}^{\infty} \rho^n_{gs}(\lambda) \log(n(\epsilon'_n(\lambda)));$$

$$E_{gs} = \sum_{n=0}^{\infty} \int d\lambda \epsilon_{0n}(\lambda) \rho_{gs}^{n}(\lambda);$$
$$\rho_{gs}^{n}(\lambda) = \delta_{n1} \int \frac{dk}{2\pi} s(\lambda - g(k)) + \frac{1}{L} D_n(\lambda). \tag{A11}$$

Here E_{gs} is the ground state energy of the system.

One now wants to consider how Ω behaves at $T \to 0$. If one can show that the leading order correction in Ω at low temperatures is T^2 then as $S = -\partial_T \Omega$ one will have shown that the entropy vanishes as $T \to 0$, and so the ground state of the system is a singlet.

In order to see that Ω has no term linear in T, it is sufficient to consider the zero temperature values of the energies, $\epsilon(k)$ and $\epsilon'_n(\lambda)$. At the particle-hole symmetric point, one has

$$\epsilon(k, T=0) > 0 \ , \text{ for all k;}$$
$$\epsilon'_1(\lambda, T=0) < 0 \ , \text{ for all } \lambda;$$
$$\epsilon'_n(\lambda, T=0) = 0 \ , \ n > 1, \text{ for all } \lambda. \tag{A12}$$

If one substitutes these expressions into the expression for Ω and uses the fact that $\int d\lambda \rho_{gs}^{n}(\lambda) = 0$, $n > 1$, one sees that $\Omega = E_{gs} + \mathcal{O}(T^2)$.

Now if one is away from the particle-hole symmetric point, one has instead

$$\epsilon(k, T=0) > 0 \ , \text{ for all k;}$$
$$\epsilon'_n(\lambda, T=0) = n(\frac{U_1}{2} + \epsilon_1) \ , \text{ for all } \lambda. \tag{A13}$$

Now while $\epsilon'_1(\lambda)$ is neither solely positive nor solely negative at zero temperature, its leading order finite temperature correction is (see Section 8.3.7 of Ref. 42),

$$\epsilon'_1(\lambda, T) = \epsilon'_1(\lambda, T=0) + \mathcal{O}(T^2). \tag{A14}$$

Substituting these forms of the energies into the expression for the free energy, one again sees that there is no term in Ω that is linear in T.

Appendix B: Derivation of the Conductance in SBMFT

Here we present a derivation of the conductance in the general case of asymmetrically coupled dots. To determine the conductance we solve the one-particle Schrödinger equation of the SBMFT Hamiltonian, $H_{SBMFT}|\psi\rangle = E|\psi\rangle$ where $|\psi\rangle$ equals

$$|\psi > = \int_{-\infty}^{+\infty} dx g_1(x) c_1^{\dagger}(x)|0> + \int_{-\infty}^{+\infty} dx g_2(x) c_2^{\dagger}(x)|0> + \epsilon_1 d_1^{\dagger}|0> + \epsilon_2 d_2^{\dagger}|0> . \tag{B1}$$

This gives the following four equations:

$$-i\partial_x g_1(x) + \epsilon_1 \tilde{V}_{11}\delta(x) + \epsilon_2 \tilde{V}_{12}\delta(x) = E g_1(x); \tag{B2}$$
$$-i\partial_x g_2(x) + \epsilon_1 \tilde{V}_{21}\delta(x) + \epsilon_2 \tilde{V}_{22}\delta(x) = E g_2(x); \tag{B3}$$
$$(\tilde{\epsilon}_{d_1} - E)\,\epsilon_1 + \tilde{V}_{11} g_1(0) + \tilde{V}_{21} g_2(0) = 0; \tag{B4}$$
$$(\tilde{\epsilon}_{d_2} - E)\,\epsilon_2 + \tilde{V}_{22} g_2(0) + \tilde{V}_{12} g_1(0) = 0. \tag{B5}$$

We then take the functions $g_{1,2}(x)$ found in the one particle wavefunction $|\psi\rangle$ to be of the following form:

$$g_1(x) = e^{iEx}\left(\theta(-x) + R_{11}\theta(x)\right); \tag{B6}$$
$$g_2(x) = e^{iEx}\theta(x) T_{12}. \tag{B7}$$

Substituting the ansatz (Eqns. B6 and Eq. B7) into the above four equations, we obtain four equations from which one can solve for T_{12}. The conductance G, equal to $G = \frac{2e^2}{h} T_{12} T_{12}^*$, is then

$$\begin{aligned} G &= \frac{2e^2}{h}\frac{N}{D} \\ N &= 16\left[\tilde{V}_{12}\tilde{V}_{22}\tilde{\epsilon}_{d_1} + \tilde{V}_{11}\tilde{V}_{21}\tilde{\epsilon}_{d_2}\right]^2 \\ D &= 8\left[\tilde{V}_{11}\tilde{V}_{12} + \tilde{V}_{21}\tilde{V}_{22}\right]^2 \tilde{\epsilon}_{d_1}\tilde{\epsilon}_{d_2} + 16\tilde{\epsilon}_{d_1}^2\tilde{\epsilon}_{d_2}^2 + \left[\tilde{V}_{12}\tilde{V}_{21} - \tilde{V}_{11}\tilde{V}_{22}\right]^4 \\ &\quad + 4\tilde{\epsilon}_{d_1}^2\left[\tilde{V}_{12}^2 + \tilde{V}_{22}^2\right]^2 + 4\tilde{\epsilon}_{d_2}^2\left[\tilde{V}_{11}^2 + \tilde{V}_{21}^2\right]^2. \end{aligned} \tag{B8}$$

We have also computed the transmission amplitude using Ref. 50:

$$T = \mathrm{Tr}\left\{G^a \tilde{\Gamma}_R G^r \tilde{\Gamma}_L\right\}, \tag{B9}$$

where $G^{a/r}$ are advanced and retarded Green's function matrix and $\tilde{\Gamma}_R$ and $\tilde{\Gamma}_L$ are defined by

$$\tilde{\Gamma}_R = \begin{bmatrix} \tilde{V}_{21}^2 & \tilde{V}_{21}\tilde{V}_{22} \\ \tilde{V}_{21}\tilde{V}_{22} & \tilde{V}_{22}^2 \end{bmatrix}, \qquad \tilde{\Gamma}_L = \begin{bmatrix} \tilde{V}_{11}^2 & \tilde{V}_{11}\tilde{V}_{12} \\ \tilde{V}_{11}\tilde{V}_{12} & \tilde{V}_{12}^2 \end{bmatrix}. \tag{B10}$$

We find that this trace formula (Eq. B9) gives exactly the same result.

Appendix C: SBMFT for double dots in the symmetric case

In this appendix we review the SBMFT approach for the symmetric case ($\epsilon_{d1} = \epsilon_{d2} \equiv \epsilon_d$). In this limit, the mean field equations (Eq. 7 and Eq. 8) reduce to

$$\begin{aligned} \sum_\sigma \langle f_\sigma^\dagger(t) f_\sigma(t)\rangle + r^2 &= 1; \\ \sqrt{2}\tilde{V}\mathrm{Re}[\sum_{k,\sigma}\langle c_{ke\sigma}^\dagger(t) f_\sigma(t)\rangle] + i\lambda r^2 &= 0. \end{aligned} \tag{C1}$$

The above equations can be equivalently written as

$$\begin{aligned} \frac{1}{2\pi}\sum_\sigma \int d\omega \langle f_\sigma^\dagger(\omega) f_\sigma(\omega)\rangle + r^2 &= 1; \\ \frac{\sqrt{2}\tilde{\mathrm{V}}}{2\pi}\mathrm{Re}\left[\sum_\sigma \int d\omega \left\langle c_{ke\sigma}^\dagger(\omega) f_\sigma(\omega)\right\rangle\right] + i\lambda r^2 &= 0. \end{aligned} \tag{C2}$$

The correlation functions are computed to be

$$\begin{aligned} \langle f_\sigma^\dagger(\omega) f_\sigma(\omega)\rangle &= \frac{2\tilde{\Delta}}{(k-\tilde{\epsilon}_d)^2 + 4\tilde{\Delta}^2} f(\omega) \\ \langle c_{ke\sigma}^\dagger(\omega) f_\sigma(\omega)\rangle &= \frac{\sqrt{2}\tilde{V}}{k - \tilde{\epsilon}_d - 2i\tilde{V}^2} f(\omega) \end{aligned} \tag{C3}$$

where $f(\omega)$ is the Fermi function. Upon substituting these expressions for correlation functions the mean field equations read

$$\begin{aligned} \frac{\tilde{\Delta}}{\Delta} - 1 + \frac{1}{\pi}\arctan[\frac{2\cdot\tilde{\Delta}}{\tilde{\epsilon}_d}] &= 0; \\ \frac{\tilde{\epsilon}_d - \epsilon_d}{\Delta} + \frac{1}{\pi}\log[\frac{(\tilde{\epsilon}_d^2 + 4\cdot\tilde{\Delta}^2)}{D^2}] &= 0. \end{aligned} \tag{C4}$$

Notice that the SBMFT equations (Eqs. C4) for double dots are strikingly similar to the single-dot case (see Eqns. 7.99 and 7.100 of Ref. 47). However it is this slight difference in coefficients that force the conductance to vanish in the Kondo regime of the dot. To show this, we note that the conductance in the symmetric limit reduces to (compare Eqn. B8)

$$G = 2\frac{e^2}{h}\frac{4\tilde{\Delta}^2}{4\tilde{\Delta}^2 + \tilde{\epsilon}_d^2}. \tag{C5}$$

In the Kondo limit, $\tilde{\Delta} \to 0$ and hence the second equation in C4 becomes

$$\tan^{-1}\left(\frac{2\tilde{\Gamma}}{\tilde{\epsilon}_d}\right) = \pi. \tag{C6}$$

(If this was a single dot the r.h.s of this would read $\pi/2$.) This in turn implies that $\tilde{\Gamma}/\tilde{\epsilon}_d$ goes to 0 in the Kondo limit which finally implies that the conductance does indeed go to zero in the Kondo limit so satisfying the Friedel sum rule. Parenthetically, we note that Eqn. C6 implies that the correct branch-cut for arctangent is $\tan^{-1} x = \pi + \mathrm{PV}\left[\tan^{-1} x\right]$ where PV denotes the principle value of arctangent restricted to the domain $[-\frac{\pi}{2}, \frac{\pi}{2}]$.

We end by checking that more complicated dot Hamiltonians also obey the Friedel sum rule. To this end we consider allowing interdot tunneling. With the presence of the term $t_c d_1^\dagger d_2 + \text{h.c.}$ in the Hamiltonian, the expressions for the correlation functions, dot occupancy and the conductance are slightly modified. Defining the renormalized tunneling as $\tilde{t}_c = t_c r_1 r_2$ we find,

$$\langle f_\sigma^\dagger(\omega) f_\sigma(\omega)\rangle = \frac{2\tilde{\Delta}}{\left(\omega - \tilde{\epsilon}_d - \tilde{t}_c\right)^2 + 4\tilde{\Delta}^2} f(\omega); \tag{C7}$$

$$\langle c_{ke\sigma}^\dagger(\omega) f_\sigma(\omega)\rangle = \frac{\sqrt{2}\tilde{V}}{\omega - \tilde{\epsilon}_d - \tilde{t}_c - 2i\tilde{V}^2} f(\omega). \tag{C8}$$

The expression for total dot occupancy is

$$n_d = \frac{2}{\pi}\arctan\left[\frac{2\tilde{\Delta}}{\tilde{\epsilon}_d + \tilde{t}_c}\right]. \tag{C9}$$

The conductance can be computed by extending the method outlined in Appendix B, so obtaining

$$G = 2\frac{e^2}{h}\frac{4\tilde{\Delta}^2}{4\tilde{\Delta}^2 + \left(\tilde{\epsilon}_d + \tilde{t}_c\right)^2}. \tag{C10}$$

It is trivial to check from Eqn. C9 and Eqn. C10 that the Friedel sum rule remains satisfied for finite t_c, i.e., $G = 2\frac{e^2}{h}\sin^2\left[\frac{\pi n_d}{2}\right]$.

---

[1] D. Goldhaber-Gordon et al., Phys. Rev. Lett. **81**, 5225 (1998); D. Goldhaber-Gordon et al., Nature **391**, 156 (1998).
[2] S. Cronenwett et al., Science **540**, 281 (1998); W. G. van der Wiel et al., Science **289**, 2105 (2000).
[3] R. M. Potok, I. G. Rau, H. Shtrikman, Y. Oreg, D. Goldhaber-Gordon, Nature **446**, 167 (2007).
[4] C. H. L. Quay, John Cumings, Sara Gamble, R. de Picciotto, H. Kataura, D. Goldhaber- Gordon, Phys. Rev. B 76, 245311 (2007).
[5] Minchul Lee, Mahn-Soo Choi, Rosa Lopez, Ramon Aguado, Jan Martinek, and Rok Zitko, Phys. Rev. B **81**, 121311 (2010).
[6] Eran Sela and Ian Affleck, Phys. Rev. Lett. **103**, 087204 (2009).
[7] Eran Sela and Ian Affleck, Phys. Rev. Lett. **102**, 047201 (2009).
[8] Ireneusz Weymann, Phys. Rev. B **78**, 045310 (2008).
[9] Justin Malecki, Eran Sela, and Ian Affleck, arXiv:1009.0860 (2010).
[10] Yunori Nisikawa and Akira Oguri,J. Phys.: Conf. Ser. **150**,022066 (2009).
[11] R. M. Konik, Phys. Rev. Lett. **99**, 076602 (2007).
[12] R. M. Konik, New J. Phys. **9**, 257 (2007).
[13] R. Zitko and J. Bonca, Phys. Rev. B **76**, 241305(R) (2007).

[14] Rok Zitko and Janez Bonca, Phys. Rev. B **74**, 045312 (2006).
[15] Chung-Hou Chung and W. Hofstetter, Phys. Rev. B **76**, 045329 (2007).
[16] G.-H. Ding, Fei Ye, and B. Dong, J. Phys. Cond.-Matt. **21**, 455303 (2009).
[17] Ding Guo-Hui and Ye Fei, Chin. Phys. Lett. **24**, 2926 (2007).
[18] R. Lopez, D. Sanchez, M. Lee, M.-S. Choi, P. Simon, and K. Le Hur, Phys. Rev. B 71, 115312 (2005).
[19] E. Vernek, N. Sandler, S.E. Ulloa, and E.V. Anda, Physica E **34**, 608 (2006).
[20] Guo-Hui Ding, Chul Koo Kim, and Kyun Nahm, Phys. Rev. B **71**, 205313 (2005).
[21] Luis G. G.V. Dias da Silva, Nancy P. Sandler, Kevin Ingersent, and Sergio E. Ulloa, Phys. Rev. Lett. **97**, 096603 (2006).
[22] Luis G. G. V. Dias da Silva, Kevin Ingersent, Nancy Sandler, and Sergio E. Ulloa1, Phys. Rev. B **78**, 153304 (2008).
[23] Eran Sela and Ian Affleck, Phys. Rev. B **79**, 125110 (2009).
[24] J. P. Dahlhaus, S. Maier, and A. Komnik, Phys. Rev. B **81**, 075110 (2010).
[25] J. C. Chen, A.M. Chang, and M. R. Melloch, Phys. Rev. Lett. **92**, 176801 (2004).
[26] M. Sigrist, A. Fuhrer, T. Ihn, K. Ensslin, S. E. Ulloa, W.Wegscheider, and M. Bichler, Phys. Rev. Lett. **93**, 066802 (2004).
[27] A M Chang and J C Chen, Rep. Prog. Phys. **72**, 096501 (2009).
[28] A. W. Holleitner, A. Chudnovskiy, D. Pfannkuche, K. Eberl, and R. H. Blick, Phys. Rev. B **70**, 075204 (2004).
[29] A. Hubel, K. Held, J. Weis, and K. v. Klitzing, Phys. Rev. Lett. **101**, 186804 (2008).
[30] A. Posazhennikova and P. Coleman, Phys. Rev. Lett. **94**, 036802 (2005).
[31] R. M. Konik, H. Saleur, and A.W.W. Ludwig, PRL **87**, 236801 (2001); ibid, PRB **66**, 125304 (2002).
[32] Y. Tanaka and N. Kawakami, Phys. Rev. B **72**, 085304 (2005).
[33] A. A. Gogolin, R. M. Konik, H. Saleur, and A. W. W. Ludwig, Ann. Phys. (Leipzig) 16, 678 (2007).
[34] D. M. Newns and N. Read, Advances in Physics **36**, 799 (1987).
[35] A. A. Aligia and L. A. Salguero, Phys. Rev. B **70**, 075307 (2004).
[36] K. Kang, S. Y. Cho, J.-J. Kim, and S.-C. Shin, Phys. Rev. B **63**, 113304 (2001).
[37] L. H.C.M. Nunes, M. Figueira, M. Foglio, Phys. Lett. A **358**, 313 (2006).
[38] P. Schlottmann, Phys. Rev. B **65**, 024431 (2001).
[39] J. Kroha, P. J. Hirschfeld, K. A. Muttalib, and P. Wölfle, Solid States Communications **83**, 1003 (1992).
[40] P. Wölfle, J. Low Temp. Phys. **99**, 625 (1995).
[41] M. Pustilnik and L.I. Glazman, Phys. Rev. Lett. **87**, 216601 (2001).
[42] A. Tsvelik and P. Wiegmann, Adv. in Phys. **32** (1983) 453.
[43] P. Wiegmann, V. Filyov, and A. Tsvelik, Sov. Phys. JETP Lett. **35** (1982) 77; N. Kawakami and A. Okiji, Phys. Lett. A **86**, 483 (1981).
[44] D. Langreth, Phys. Rev. **150**, 516 (1966).
[45] R. M. Fye, Phys. Rev. B **41**, 2490 (1990).
[46] T. Costi, A. Hewson, and V. Vlatic, J. Phys.: Cond. Mat. **6**, 2519 (1994).
[47] A. Hewson, *The Kondo Problem to Heavy Fermions*, Cambridge University Press, Cambridge, UK (1993).
[48] H. R. Krishnamurthy, J. W. Wilkins, and K. G. Wilson, Phys. Rev. B. **21**, 1003 (1980).
[49] K. G. Wilson, Rev. Mod. Phys. **47**, 773 (1975).
[50] Y. Meir and N.S Wingreen, Phys. Rev. Lett. **68**, 2512 (1992).